Received May 22, 2018, accepted July 9, 2018, date of publication July 25, 2018, date of current version August 20, 2018.

*Digital Object Identifier 10.1109/ACCESS.2018.2859805*

# A Robust Incremental-Quaternion-Based Angle and Axis Estimation Algorithm of a Single-Axis Rotation Using MARG Sensors

**XIAOLONG XU, XINCHENG TIAN, AND LELAI ZHOU, (Member, IEEE)**
School of Control Science and Engineering, Robotics Research Center, Shandong University, Jinan 250061, China

Corresponding author: Xincheng Tian (txch@sdu.edu.cn)

This work was supported in part by the National Key Research and Development Program of China under Grant 2017YFF0107803 and in part by the National Natural Science Foundation of China under Grant 61603216.

**ABSTRACT** A robust incremental-quaternion-based algorithm is proposed in this paper to estimate the angle and the axis of a single-axis rotation whose rotation axis is invisible or inaccessible. We establish a model to estimate the rotation angle and axis according to the relationship between the incremental quaternion and the pair of rotating axis and angles. Moreover, the solutions for the model are detailedly described in this paper. This algorithm could achieve full range of rotation angle and all-attitude rotation axis measurements with high-computational efficiency. It has good performances in the rotation angle and axis estimation no matter whether the measured target is in dynamic or static movement, which solves the inaccurate rotating-axis attitude problem in other methods when the target is doing low-speed rotation. Using the designed measurement unit based on magnetic, angular rate, and gravity sensors, this algorithm eliminates the drift of measurement results caused by the integral error of the gyroscope. The effectiveness of this algorithm has been validated through a single-axis motion control platform by comparing with another two methods. Results show that the proposed algorithm provides a more accurate estimation of rotation angle and the axis of a single-axis rotation of high or low speed.

**INDEX TERMS** Incremental quaternion, angle and axis estimation, single-axis rotation, MARG sensors.

## I. INTRODUCTION

The accurate angle and axis measurements of a single-axis rotation are important bases in robots [1], engineering applications [2], spacecraft [3], inertial navigation [4], [5] and medical rehabilitation [6]. However, the electrical and mechanical properties of angular sensors will gradually change due to the components aging or some uncontrollable influences such as collision, which could cause the unreliable measurement of angular displacement. Therefore, it is necessary to regularly calibrate the angular sensors using the specific calibration system. For instance, to ensure the flight safety, it is of great importance to calibrate the rotation angles of the ailerons, elevators and rudders before the aircraft takes off. In order to enable real-time estimation and tracking of rotation angles and axis, it is necessary to develop the easy and reliable estimation system as well as accurate and efficient estimation algorithms.

At present, there are many kinds of methods for rotation angle measurements, such as the mechanical methods [7], electromagnetic methods [8], vision-based methods [9] and inertial- measurement-unit (IMU)-based methods [10]. In the mechanical methods, the measured equipment is required to modify the mechanical structure. The electromagnetic methods need previous complex installation and calibration [11]. Both of them could only be utilized in the systems with known rotation axis. The vision methods rely on some special equipment with complicated installation and test process as well as complicated computation [12]. Using IMU-based methods to estimate the rotation angles and axis attitude of the single-axis rotation is a relatively new field. Owing to the small size, low cost, ease of integration and strong adaptability of inertial sensors, inertial-sensors-based motion tracking system has become a meaningful research. This motion tracking system can be divided into IMU-based and MARGs-based systems according to the presence or absence of the magnetometer. The IMU, composed of a triaxial accelerometer and a triaxial gyroscope, could observe the angular velocity and acceleration of the target in three-dimensional space. It could be applied to devices that require attitudes for precise positioning such as mobile robots, unmanned underwater vehicles (UAVs) and spacecraft inertial navigation devices [13]–[15]. A MARG system includes an IMU and

a triaxial magnetometer. Compared to the IMU, the MARG system uses the magnetic field as a reference in addition to the gravity field, which provides a more accurate measurement. The MARG sensors are adopted in this work to estimate the rotation angle and axis attitude of a single-axis rotation.

An accurate and efficient algorithm is the soul of rotation angle and axis estimation. There are many methods to estimate the orientation, such as Kalman filter (KF) [16], extend Kalman filter (EKF) [17], unscented Kalman filter (UKF) [18] and particle Kalman filter (PKF) [19]. The gradient descent method [20] and complementary filtering algorithm [21] are widely used in motion tracking systems due to advantages of simple structure, quick implementation and high computational efficiency. However, the above methods simply obtain the attitude of the measured target in forms of quaternion or Euler angles instead of the rotation angles or axes of the measured target. A few of the existing methods rely heavily on the rotation axis to measure the rotation angles [22], [23]. The rotation axis is usually unknown or difficult to measure in some systems, which induces a poor accuracy of rotation angles measurement in those methods. For instance, when the measured target has a curve surface with no horizontal or right-angle surfaces, it is difficult and complicated to install the measurement equipment, which leads to a difficult or inaccessible measurement of the rotation axis. Tomazic and Stancin proposed the gyroscope-based simultaneous orthogonal rotations angle (SORA) method. It uses a triaxial gyroscope to measure the rotation angle when the angular velocities of the target are approximately constant [24]. The SORA method is simple and suitable for real-time estimation of rotation angles in low-cost applications. However, the zero drift of gyroscopes will lead to accumulated errors in the angle and axis estimation after a long working period. Zheng *et al*. proposed an IMU-based method to measure the angle of a single-axis rotation when the target is at high angular velocity [10]. This method utilizes the angular velocities of an IMU to calculate orientation of the rotating axis. The rotation matrix is obtained by computing the Euler angles of the target in initial and ending positions. An equation is developed to describe the relationship between the rotation matrix inferred by Euler angles and rotation angles. An interpolation algorithm is utilized to solve this equation to get the rotation angles. This method could not achieve full-range rotation angle and all-attitude rotation axis measurements due to the gimbal lock problem existed in the Euler angles. It also heavily relies on the accuracy of the gyroscope during the measurement process, which limits the measurement accuracy of the rotation angle and axis when the target is in low-speed rotation.

In order to solve the mentioned problems existing in the rotation angle and axis measurements, an incremental-quaternion-based angle and axis estimation algorithm is proposed in this work to measure the single-axis rotation with unknown rotation axis using MARG sensors. Meanwhile, a MARGs-based measurement unit is designed in this work with the size of 30mm × 30mm × 10mm. It has a separate power supply system and the information from MARG sensors could be transmitted to the host via WiFi. The proposed method has no restriction on the installation accuracy which simplifies the installation and measurement processes. It calculates the rotation angles and axis attitude through the incremental quaternion determined by the angular rate, acceleration and magnetic information, which could achieve full-angle and all-attitude rotating-axis measurements. It has the advantages of high computational efficiency and good real-time performance dynamically and statically, which lead to an easy implementation in the embedded systems.

This paper is organized as follows. Section II describes the preliminaries and problem statement. The detailed model and derivation of the proposed algorithm are explained in Section III. Section IV introduces the developed MARGs-based measurement unit. The dynamic and static experiments as well as results are presented in Section V. Section VI concludes this work with a short summary.

A notation system of leading super-scripts and sub-scripts adopted from Craig [25] is used to denote the relative coordinates of orientations and vectors. A leading superscript denotes the frame to be described and a leading subscript denotes the frame this is with reference to. For instance, ${}^{A}_{B}\mathbf{C}$ is the transformation matrix of frame $\{A\}$ relative to frame $\{B\}$ and ${}^{A}\mathbf{v}$ is a vector in frame $\{A\}$.

## II. PRELIMINARIES AND PROBLEM FORMULATION

### A. PRELIMINARIES

A quaternion, composed of a four-dimensional complex number, could be used to represent the attitude of a rigid body or frame in three-dimensional space. If a frame $\{B\}$ is obtained by performing a limited number of rotations on the frame $\{A\}$, it can be achieved by a single $\theta$-degrees rotation around a unit rotation vector ${}^{A}\mathbf{v} = [v_x v_y v_z]^{\mathrm{T}}$ in frame $\{A\}$, as shown in Fig. 1, where the mutually orthogonal unit vectors ${}^{A}\mathbf{X}$, ${}^{A}\mathbf{Y}$, and ${}^{A}\mathbf{Z}$ as well as ${}^{B}\mathbf{X}$, ${}^{B}\mathbf{Y}$ and ${}^{B}\mathbf{Z}$ are the main axes in frames $\{A\}$ and $\{B\}$, respectively.

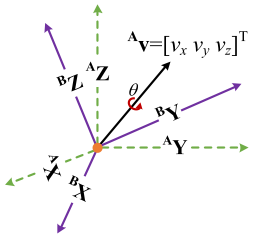


**FIGURE 1.** The $\theta$-degrees rotation around axis ${}^{A}\mathbf{v}$ from frame $\{A\}$ to frame $\{B\}$.

The rotation in Fig. 1 can be expressed in a normalized quaternion ${}^{B}_{A}\mathbf{q}$ which has the following relationship with ${}^{A}\mathbf{v}$ [26].

$$\begin{aligned} {}^{B}_{A}\mathbf{q} &= [\, q_1 \quad q_2 \quad q_3 \quad q_4 \,]^{\mathrm{T}} \\ &= [\, \cos\frac{\theta}{2} \quad v_x \sin\frac{\theta}{2} \quad v_y \sin\frac{\theta}{2} \quad v_z \sin\frac{\theta}{2} \,]^{\mathrm{T}} \end{aligned} \tag{1}$$

In this paper, we use ${}^{B}_{A}\mathbf{q}^{*}$ represents the conjugate of ${}^{B}_{A}\mathbf{q}$, as in (2) [26], which describes the reverse rotation of the same attitude.

$$ {}^{B}_{A}\mathbf{q}^{*} = {}^{A}_{B}\mathbf{q} = \begin{bmatrix} q_1 & -q_2 & -q_3 & -q_4 \end{bmatrix}^{\mathrm{T}} \tag{2} $$

The product of quaternions in (3) follows the Hamilton principle [27], which could convert multiple consecutive rotations into one rotation as in (4). The rotation axis of the rotations should be represented in the original frames, namely, the quaternion should be generated by the non-mapping operation. Note that the product of quaternions does not satisfy the multiplicative exchange principle.

$$ \begin{aligned} \mathbf{a} \otimes \mathbf{b} &= \begin{bmatrix} a_1 & a_2 & a_3 & a_4 \end{bmatrix}^{\mathrm{T}} \otimes \begin{bmatrix} b_1 & b_2 & b_3 & b_4 \end{bmatrix}^{\mathrm{T}} \\ &= \begin{bmatrix} a_1b_1 - a_2b_2 - a_3b_3 - a_4b_4 \\ a_1b_2 + a_2b_1 + a_3b_4 - a_4b_3 \\ a_1b_3 - a_2b_4 + a_3b_1 + a_4b_2 \\ a_1b_4 + a_2b_3 - a_3b_2 + a_4b_1 \end{bmatrix} \end{aligned} \tag{3} $$

$$ {}^{C}_{A}\mathbf{q} = {}^{C}_{B}\mathbf{q} \otimes {}^{B}_{A}\mathbf{q} \tag{4} $$

### B. PROBLEM FORMULATION

In this paper, an incremental-quaternion-based angle and axis estimation algorithm is proposed to measure the single-axis rotation. Fig. 2 is the schematic diagram of the rotation angle measurement in which we fixed the MARGs-based measurement unit on the surface of the target. When the target rotates around an invisible or inaccessible axis, we can resolve the rotation angle and rotating-axis attitude through the incremental quaternion from the MARGs. To describe the problem clearly, we first introduce the spatial relationship between the coordinate systems.

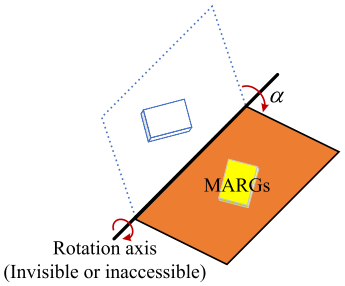


**FIGURE 2.** Schematic diagram of the rotation angle measurement.

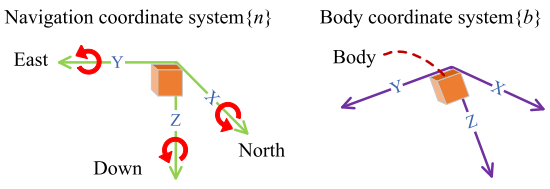


**FIGURE 3.** Coordinate systems in this work.

Fig. 3 shows the employed coordinate systems. The north-east-down (NED) frame is introduced to be the navigation frame $\{n\}$, and the body frame $\{b\}$ follows the right-hand rule with **X**-front, **Y**-right and **Z**-down. The body frame is fixed on the MARGs, whose attitude will change as the target.

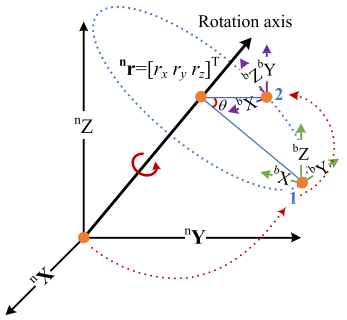


**FIGURE 4.** Schematic diagram of frame {*b*} rotating around axis in frame {*n*}.

Fig. 4 describes the problem through the relationship between frames $\{b\}$ and $\{n\}$. Assuming that a unit rotation axis ${}^{n}\mathbf{r}$ in the navigation frame has $r_x$, $r_y$ and $r_z$ components on **X**, **Y** and **Z** axis, its attitude could be described as ${}^{n}\mathbf{r} = [r_x r_y r_z]^{\mathrm{T}}$. $\theta$ is the rotation angle of frame $\{b\}$ from positions 1 to 2. ${}^{b}_{n}\mathbf{q}_i$ is the quaternion obtained from the MARGs, which describes the orientation of the frame $\{b\}$ relative to the frame $\{n\}$ at position $i$. For example, ${}^{b}_{n}\mathbf{q}_1$ and ${}^{b}_{n}\mathbf{q}_2$ are quaternions in positions 1 and 2, respectively. Through the MARGs-based measurement unit, we can obtain the quaternion ${}^{b}_{n}\mathbf{q}_i$ continuously.

Though ${}^{n}\mathbf{r}$ is fixed in the navigation frame, its attitude is unknown. The problem is how to measure the rotation angles and rotating-axis attitude of a single-axis rotation when the rotation axis is unknown. Two assumptions are given below: (1) Due to the rotation is a single-axis rotation, it is considered in this work that the rotation axis is fixed after the start of measurement and there are no other dimensions of freedoms during the rotation of the measured target. (2) The accelerometers, gyroscopes and magnetometers of the MARGs are mounted orthogonally and their corresponding axes are overlapped or parallel. The objective of this work is to propose a method to estimate the unknown parameter $\theta$ and unknown rotation axis ${}^{n}\mathbf{r}$ according to those known quaternion measurements ${}^{b}_{n}\mathbf{q}_i (i = 1, 2, \ldots, n)$ by MARGs.

## III. MODEL AND DERIVATION

### A. MODEL ESTABLISHMENT

In this section, we present a detailed derivation of the model to measure the rotation angle and axis using incremental quaternion when the rotation axis is unknown or inaccessible. We define the incremental quaternion ${}^{n}\mathbf{q}_{\Delta}$ from positions 1 to 2 has the form in (5), where the second subscript number represents the order of elements in it.

$$ \begin{aligned} {}^{n}\mathbf{q}_{\Delta} &= \begin{bmatrix} {}^{n}q_{\Delta,1} & {}^{n}q_{\Delta,2} & {}^{n}q_{\Delta,3} & {}^{n}q_{\Delta,4} \end{bmatrix}^{\mathrm{T}} \\ &= \begin{bmatrix} \cos\dfrac{\theta}{2} & {}^{n}r_x \sin\dfrac{\theta}{2} & {}^{n}r_y \sin\dfrac{\theta}{2} & {}^{n}r_z \sin\dfrac{\theta}{2} \end{bmatrix}^{\mathrm{T}} \end{aligned} \tag{5} $$

According to outputs of MARG sensors, we can obtain the quaternions ${}^b_n\mathbf{q}_1$ and ${}^b_n\mathbf{q}_2$, respectively [28]. For clarity, we show their forms in (6) and (7).

$$ {}^b_n\mathbf{q}_1 = \begin{bmatrix} {}^b_nq_{1,1} & {}^b_nq_{1,2} & {}^b_nq_{1,3} & {}^b_nq_{1,4} \end{bmatrix}^{\mathrm{T}} \tag{6} $$

$$ {}^b_n\mathbf{q}_2 = \begin{bmatrix} {}^b_nq_{2,1} & {}^b_nq_{2,2} & {}^b_nq_{2,3} & {}^b_nq_{2,4} \end{bmatrix}^{\mathrm{T}} \tag{7} $$

The frame $\{b\}$ can reach position 2 after two rotations. For simplicity, we define the first rotation is rotating the frame $\{b\}$ from a position in frame $\{n\}$ to position 1 through ${}^b_n\mathbf{q}_1$. In the second rotation, the frame $\{b\}$ is rotated from positions 1 to 2 through the incremental quaternion ${}^n\mathbf{q}_\Delta$. According to the synthesis rules of quaternions, we can get

$$ {}^b_n\mathbf{q}_2 = {}^n\mathbf{q}_\Delta \otimes {}^b_n\mathbf{q}_1 \tag{8} $$

thus, the incremental quaternion can be calculated by

$$ {}^n\mathbf{q}_\Delta = {}^b_n\mathbf{q}_2 \otimes {}^b_n\mathbf{q}_1^{-1} \tag{9} $$

According to (3), (6), and (7), the incremental quaternion has the form of

$$ {}^n\mathbf{q}_\Delta = \begin{bmatrix} {}^b_nq_{2,1}{}^b_nq_{1,1} + {}^b_nq_{2,2}{}^b_nq_{1,2} + {}^b_nq_{2,3}{}^b_nq_{1,3} + {}^b_nq_{2,4}{}^b_nq_{1,4} \\ -{}^b_nq_{2,1}{}^b_nq_{1,2} + {}^b_nq_{2,2}{}^b_nq_{1,1} - {}^b_nq_{2,3}{}^b_nq_{1,4} + {}^b_nq_{2,4}{}^b_nq_{1,3} \\ -{}^b_nq_{2,1}{}^b_nq_{1,3} + {}^b_nq_{2,2}{}^b_nq_{1,4} + {}^b_nq_{2,3}{}^b_nq_{1,1} - {}^b_nq_{2,4}{}^b_nq_{1,2} \\ -{}^b_nq_{2,1}{}^b_nq_{1,4} - {}^b_nq_{2,2}{}^b_nq_{1,3} + {}^b_nq_{2,3}{}^b_nq_{1,2} + {}^b_nq_{2,4}{}^b_nq_{1,1} \end{bmatrix} \tag{10} $$

However, due to the existed rounding errors during the computational process, the incremental quaternion ${}^n\mathbf{q}_\Delta$ needs to be normalized as a unit quaternion ${}^n\hat{\mathbf{q}}_\Delta$, which has the form of

$$ {}^n\hat{\mathbf{q}}_\Delta = \begin{bmatrix} {}^n\hat{q}_{\Delta,1} & {}^n\hat{q}_{\Delta,2} & {}^n\hat{q}_{\Delta,3} & {}^n\hat{q}_{\Delta,4} \end{bmatrix}^{\mathrm{T}} \tag{11} $$

Finally, the model to solve the rotation angle and axis of a single-axis rotation can be established as in (12). We will show the solutions in the following section.

$$ \begin{bmatrix} \cos\dfrac{\theta}{2} \\ {}^nr_x \sin\dfrac{\theta}{2} \\ {}^nr_y \sin\dfrac{\theta}{2} \\ {}^nr_z \sin\dfrac{\theta}{2} \end{bmatrix} = \begin{bmatrix} {}^n\hat{q}_{\Delta,1} \\ {}^n\hat{q}_{\Delta,2} \\ {}^n\hat{q}_{\Delta,3} \\ {}^n\hat{q}_{\Delta,4} \end{bmatrix} \tag{12} $$

### B. SOLUTIONS OF ROTATION ANGLE AND AXIS

#### 1) ROTATING-AXIS ATTITUDE ESTIMATION

An accurate estimation of rotating-axis is the premise of rotation angle measurement. According to the conversion relationship between axis-angle pairs and quaternions [27], (12) can be utilized to calculate the rotation angle and axis. However, the calculated accuracy of this method cannot meet the actual requirements for several reasons. On one hand, the rotation angle estimation is sensitive to the rotating-axis attitude [10]. Moreover, using one element of quaternion to calculate the rotation angle cannot fully describe the relationship between the rotation angle and quaternion. The inaccurate rotation angle will bring errors into the solutions of rotation axis. Therefore, we will describe how to reduce noise and obtain accurate rotating-axis attitude estimation in this section.

According to (12), we can get the expression of rotation angle by

$$ \alpha = 2\arccos({}^n\hat{q}_{\Delta,1}) \tag{13} $$

where $\alpha$ is utilized as an intermediate process for solving the rotating-axis attitude instead of the final estimation of rotation angle. Determined by the *arccos* function, $\alpha$ has the range of $[0,\ 2\pi]$, which lacks the other half $[-2\pi,\ 0]$ of the rotation angle. This problem can be solved by the following process. Once the measurement unit is fixed on the target surface, we can determine the sign of a component in the rotating axis attitude in the frame $\{n\}$. For instance, the rotation axis has a positive component on the Z-axis in frame $\{n\}$ as shown in Fig. 4. It is assumed in this context that ${}^nr_z > 0$ in the navigation frame. We could infer that ${}^n\hat{q}_{\Delta,4}$ has the same symbol as $sin(\alpha/2)$ according to

$$ {}^nr_z \sin\tfrac{\alpha}{2} = {}^n\hat{q}_{\Delta,4} \tag{14} $$

Since ${}^n\hat{q}_{\Delta,4}$ can be obtained through (10), it can be used to judge the range of rotation angle $\alpha$ by

$$ \begin{cases} \alpha \in \begin{bmatrix} 0 & 2\pi \end{bmatrix}, & if\ {}^n\hat{q}_{\Delta,4} \geq 0 \\ \alpha \in \begin{pmatrix} -2\pi & 0 \end{pmatrix}, & otherwise \end{cases} \tag{15} $$

Therefore, the full-range rotation angle can be calculated by

$$ \alpha = \begin{cases} 2\arccos({}^n\hat{q}_{\Delta,1}), & if\ {}^n\hat{q}_{\Delta,4} \geq 0 \\ -2\arccos({}^n\hat{q}_{\Delta,1}), & otherwise \end{cases} \tag{16} $$

Substituting (16) into (12), the rotating axis at time $t$ could be calculated by

$$ \begin{cases} {}^nr_{x,t} = \dfrac{{}^n\hat{q}_{\Delta,2}}{\sin\frac{\alpha}{2}} \\ {}^nr_{y,t} = \dfrac{{}^n\hat{q}_{\Delta,3}}{\sin\frac{\alpha}{2}} \\ {}^nr_{z,t} = \dfrac{{}^n\hat{q}_{\Delta,4}}{\sin\frac{\alpha}{2}} \end{cases} \tag{17} $$

When the rotation angle is close to zero, the estimation of rotation axis is inaccurate. It is necessary to limit the rotation angle when estimating the rotation axis. It is assumed that the rotation angle will be utilized to estimate the rotating-axis attitude when it is greater than a threshold $\xi_\alpha$. Furthermore, we utilize the mean filter to obtain the more reliable rotation axis. The average estimated rotation axis can be obtained by

$$ {}^n\mathbf{r} = \tfrac{1}{m}\textstyle\sum {}^n\mathbf{r}_t \tag{18} $$

where $m$ is the number of samples with the rotation angle greater than the selected threshold. Note that the average estimation ${}^{n}\mathbf{r}$ maybe not a unit vector, which should be normalized to be the final rotating-axis estimation.

#### 2) ROTATION ANGLE MEASUREMENT

Substituting the obtained rotating-axis attitude ${}^{n}\mathbf{r} = [{}^{n}r_x \ {}^{n}r_y \ {}^{n}r_z]^{\mathrm{T}}$ into (14), three formulas about the rotation angle can be inferred as in (19).

$$\begin{cases} \tan\frac{\theta}{2} = \dfrac{(\frac{{}^{n}\hat{q}_{\Delta,2}}{{}^{n}r_x})}{{}^{n}\hat{q}_{\Delta,1}} \\ \tan\frac{\theta}{2} = \dfrac{(\frac{{}^{n}\hat{q}_{\Delta,3}}{{}^{n}r_y})}{{}^{n}\hat{q}_{\Delta,1}} \\ \tan\frac{\theta}{2} = \dfrac{(\frac{{}^{n}\hat{q}_{\Delta,4}}{{}^{n}r_z})}{{}^{n}\hat{q}_{\Delta,1}} \end{cases} \tag{19}$$

Simplifying (19), the rotation angle can be calculated by

$$\theta = 2\arctan 2(\frac{1}{3}(\frac{{}^{n}\hat{q}_{\Delta,2}}{{}^{n}r_x} + \frac{{}^{n}\hat{q}_{\Delta,3}}{{}^{n}r_y} + \frac{{}^{n}\hat{q}_{\Delta,4}}{{}^{n}r_z}), {}^{n}\hat{q}_{\Delta,1}) \tag{20}$$

Due to the reciprocals of three components of ${}^{n}\mathbf{r}$ are involved, the rotation angle may distort when using (20). Therefore, we introduce three gains $\beta_x$, $\beta_y$ and $\beta_z$ through the threshold $\xi_r$ of rotating-axis components. The gain $\beta_x$ is defined in (21). $\beta_y$ and $\beta_z$ have the same definitions.

$$\begin{cases} \beta_x = 0, & if \ {}^{n}r_x < \xi_r \\ \beta_x = 1, & otherwise \end{cases} \tag{21}$$

By introducing the three gains, equation (20) could be converted into

$$\theta = 2\arctan 2(\frac{\beta_x\frac{{}^{n}\hat{q}_{\Delta,2}}{{}^{n}r_x} + \beta_y\frac{{}^{n}\hat{q}_{\Delta,3}}{{}^{n}r_y} + \beta_z\frac{{}^{n}\hat{q}_{\Delta,4}}{{}^{n}r_z}}{(\beta_x + \beta_y + \beta_z)}, {}^{n}\hat{q}_{\Delta,1}) \tag{22}$$

If a component does not meet the determination condition, it will be removed from the calculation formula. Namely, this equation will use more reliable rotating-axis components to estimate the final rotation angle. So far, we have got solutions for rotation angle and axis estimation of a single-axis rotation.

### C. ALGORITHM SUMMARY

In this section, we further summarize the process of the proposed incremental-quaternion-based angle and axis estimation algorithm. The specific steps are as follows.

*Step 1:* Calculate the incremental quaternion ${}^{n}\mathbf{q}_{\Delta}$ of the single rotation according to (10) using the known quaternion measurements ${}^{b}_{n}\mathbf{q}_i (i = 1, 2, \ldots, n)$ from MARGs.

*Step 2:* Compute the intermediate rotation angle $\alpha$ according to (16).

*Step 3:* Estimate the rotating-axis attitude ${}^{n}\mathbf{r}$ according to the incremental quaternion ${}^{n}\mathbf{q}_{\Delta}$ in *Step 1* and the rotation angle $\alpha$ in *Step 2*.

*Step 4:* Estimate the rotation angle $\theta$ using the calculated incremental quaternion ${}^{n}\mathbf{q}_{\Delta}$ and rotation axis ${}^{n}\mathbf{r}$ based on the method in Section III.B.2).

For simplicity, we use IOE (incremental orientation estimation) to represent the proposed method for angle and axis estimation in the following work.

## IV. MARGS-BASED MEASUREMENT UNIT DESIGN

To achieve the angle and axis estimation of the single-axis rotation, a MARGs-based measurement unit is designed in this work. Fig. 5 is the structure diagram of the designed measurement unit.

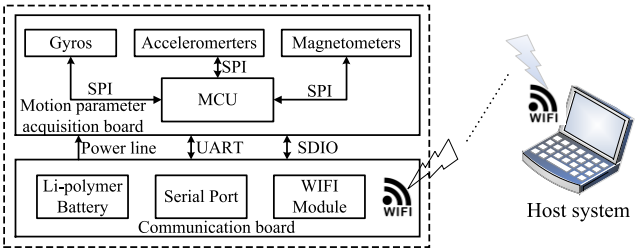


**FIGURE 5.** The structure diagram of designed measurement unit.

There are two parts in the measurement unit. One part is the motion parameter acquisition board which is used to measure the angular rate, acceleration and magnetic field information of the rotating target and then transmit them to the micro controller unit (MCU) to be analyzed and handled through the serial peripheral interface (SPI). The other is the communication board which could transmit the processed information to the host system through WiFi or serial port. There is also a lithium battery interface on the it to power the unit.

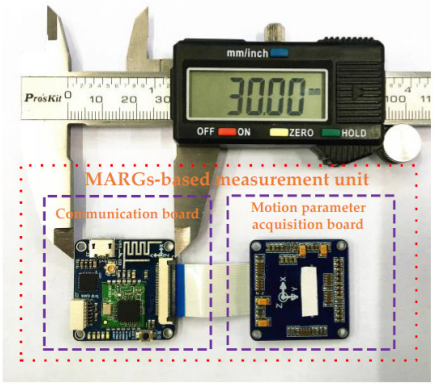


**FIGURE 6.** The MARGs-based measurement unit designed in this work.

Fig. 6 is the designed MARGs-based measurement unit in this work. With a compact size of 30mm × 30mm × 10mm, it is flexible and easy to be mounted on the surface of the measured target. The two small boards, connected by a soft cable, can be stacked together through four studs.

## V. EXPERIMENTS AND ANALYSIS

In this section, we establish a single-axis motion control platform to simulate the single-axis rotation. In order to validate the effectiveness of the IOE algorithm in estimating the angle

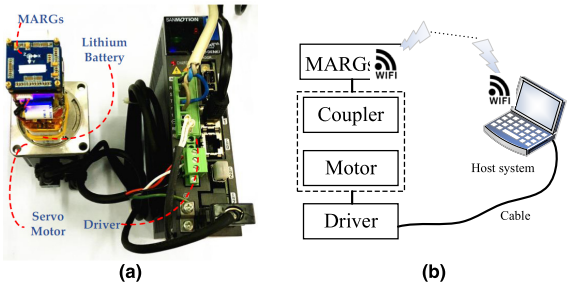


**FIGURE 7.** (a) Experiment setup; (b) Structure diagram of experiment equipment.

and axis of single-axis rotation, we design the dynamic and static experiments. In every experiment, we compare the proposed IOE algorithm with the SORA [24] and Zheng's [10] algorithms respectively based on the actual rotation angle of the motor obtained from the encoder.

### A. EXPERIMENT CONFIGURATION

Fig. 7 (a) is the established single-axis motion control platform in this work. Its structure diagram is shown in Fig. 7(b). The rotation movement is done by the servo motor according to instructions from host system. The MARGs-based measurement unit is fixed on the coupler randomly to measure the rotation angle and axis of the servo motor.

### B. DYNAMIC PERFORMANCE TEST

It is assumed in this work that the rotating object is at the dynamic state when its angular velocity is greater than 5°/s, otherwise, it is considered as static state. The reason for choosing 5°/s as the segmentation point of the dynamic and static states is that this value is far greater than the noise of gyroscope and the target moves very slowly at this speed. Furthermore, we also consider the high-speed and low-speed rotation in the dynamic and static experiments. Fig. 8 shows curves of the angle, angular velocity and angular acceleration of the servo motor in dynamic test.

The angle curve in Fig. 8(a) is obtained from the encoder. The angular velocity and angular acceleration are obtained through derivation of angle values. Therefore, there are some burrs on the two curves in Fig. 8(b) and (c), but this has no influence on the analysis of the experiment. During a period of dynamic rotation, the measured target completes four start and stop movements. The maximum forward speed of the servo motor is 234°/s, the maximum forward acceleration is 650°/ $s^2$, the maximum negative speed is −115°/s, and the maximum negative acceleration is $-600°/s^2$.

#### 1) ROTATION ANGLE MEASUREMENT RESULTS

Fig. 9 shows the estimation results of the rotation angle of four methods. Note that both the dynamic and static experiments are done 10 times, and we randomly choose one of the results to analyze. For clarity, we enlarge the part *A* in Fig. 10. It can be seen that the rotation angle computed through the

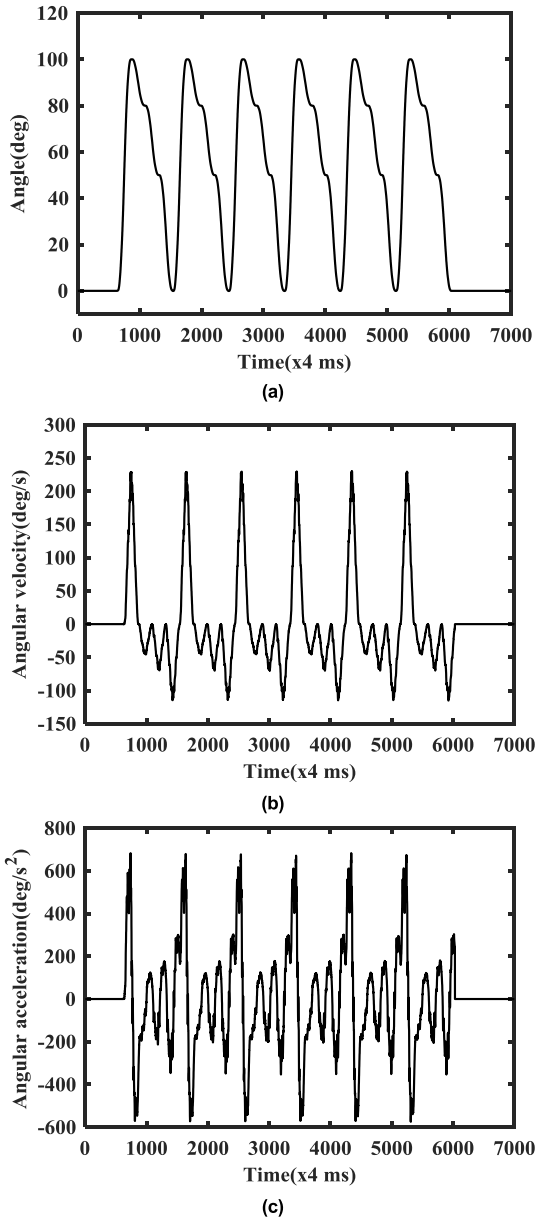


**FIGURE 8.** The angle, angular velocity and angular acceleration curves of the servo motor in dynamic experiment.

IOE algorithm is closer to the actual rotation angle of the servo motor.

Fig. 11 shows the dynamic estimation errors of rotation angle of three methods, which take the encoder outputs as references. It can be seen that the error increases as the rotation speed increases and decreases as the rotation speed decreases. There is no accumulated error in the IOE algorithm, and its maximum dynamic error is less than 2°.

#### 2) ROTATING-AXIS MEASUREMENT RESLUTS

In order to intuitively observe the estimated rotating-axis attitude, we plot the components of the rotating-axis in X, Y and Z-axis in Fig. 12. Due to the similar characteristics

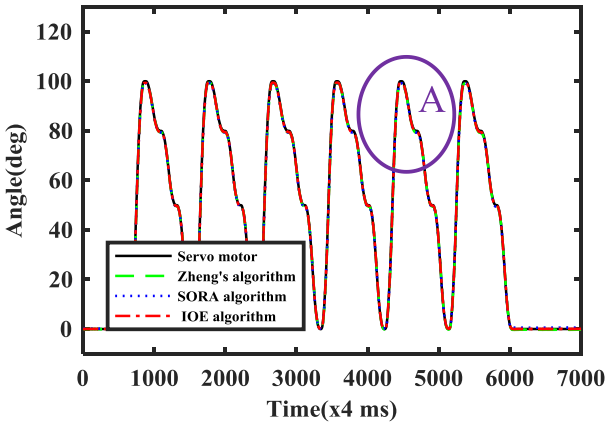


**FIGURE 9.** Estimated rotation angles in the dynamic experiment.

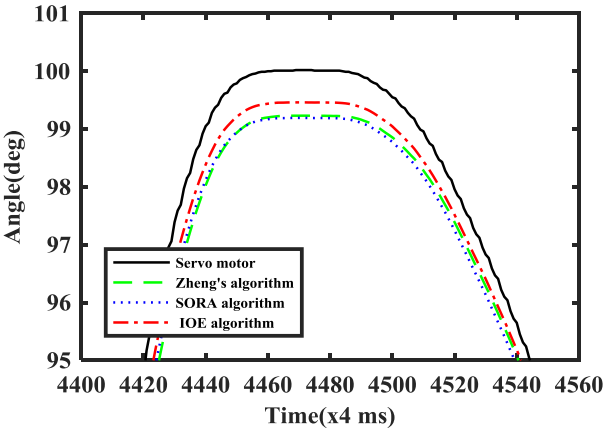


**FIGURE 10.** Magnification of part *A*.

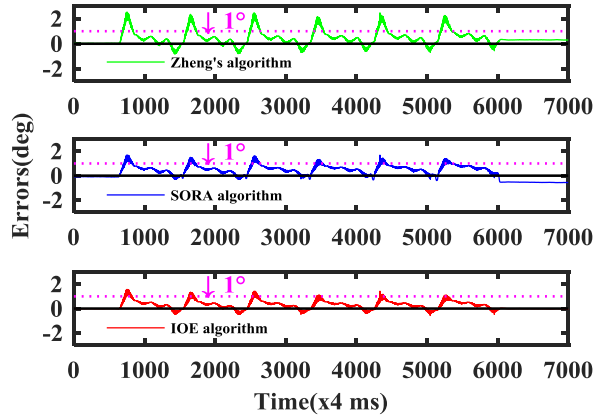


**FIGURE 11.** Dynamic estimation errors of rotation angle.

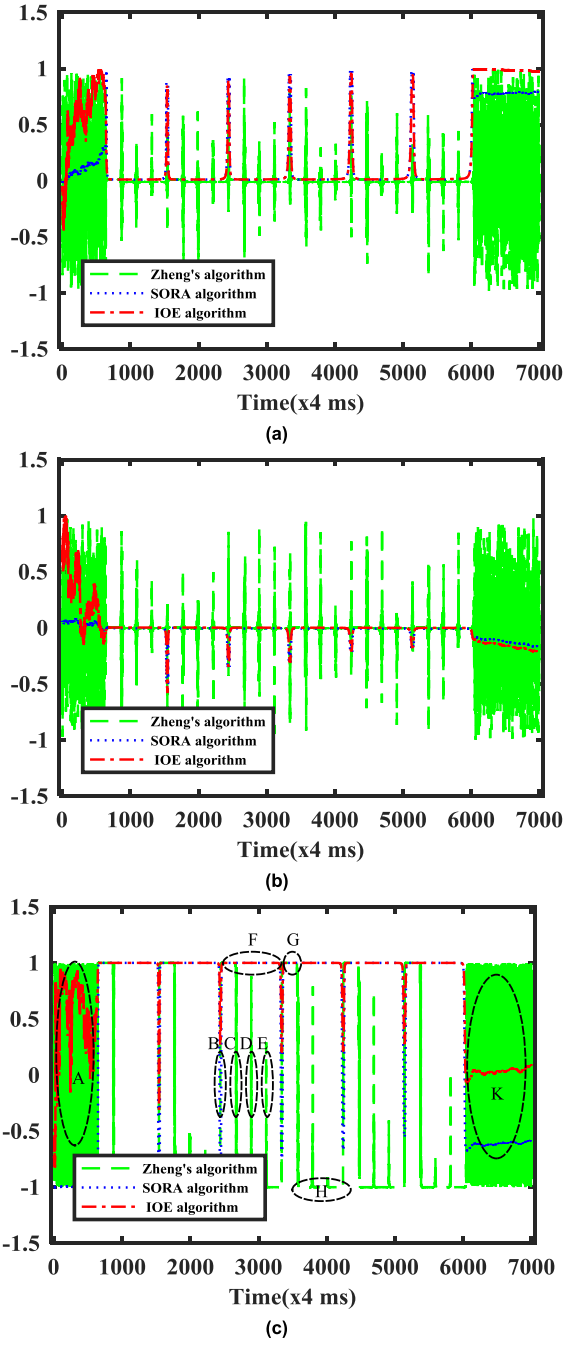


**FIGURE 12.** The estimated rotating-axis attitude in dynamic test. (a) X axis; (b) Y axis; (c) Z axis.

of three components of the rotating-axis attitude, we take the component on Z-axis as an example to analyze. The estimated rotating-axis attitudes from three methods will distort when the rotation angle is close to zero as shown in part *A, B* and *K*. This is unavoidable due to the tiny rotation angle and angular velocity make the measurement difficult for sensors. During one cycle rotation movement, when the rotation angle is greater than a value, the IOE and SORA algorithms consistently obtain a stable estimation of rotation axis as in part *F*. However, due to Zheng's algorithm relies on the angular velocities during measuring the rotating-axis attitude, the distortion will take place when the angular velocity is close to zero like parts *C*, *D* and *E*. Moreover, unlike the IOE and SORA methods, Zheng's algorithm could not response correctly to the reverse rotation of the target. For instance, the estimated rotating-axis attitudes flip at parts *G* and *H* due to the reverse velocity. However, the rotation axis does not change at that time.

We summarize the root mean square errors (RMSE) of the rotation angle and axis in the dynamic performance experiments in Table 1. The proposed IOE algorithm could achieve more accurate measurements of the rotation angle and axis with the minimum RMSE errors among three methods.

**TABLE 1. The dynamic RMSE of rotation angle and axis.**

| RMSE | Zheng's algorithm | SORA algorithm | IOE algorithm |
|---|---|---|---|
| $\theta$ | 0.465° | 0.539° | 0.299° |
| ${}^{n}r_x$ | $3.258\times10^{-3}$ | $1.087\times10^{-3}$ | $2.223\times10^{-4}$ |
| ${}^{n}r_y$ | $4.104\times10^{-3}$ | $1.621\times10^{-3}$ | $1.694\times10^{-4}$ |
| ${}^{n}r_z$ | $6.078\times10^{-5}$ | $6.041\times10^{-6}$ | $2.378\times10^{-6}$ |

### C. STATIC PERFORMANCE TEST

In the static performance experiment, the maximum angular velocity is limited to be less than $\pm5°$/s. Fig. 13 shows curves of the angle, angular velocity and angular acceleration. Due to the rotation speed is quite slow, there are large noises in the angular velocity and angular acceleration when we derivate for the angles. However, this will not affect the analysis of the performance of different methods. It can be seen from Fig. 13(b) that the maximum forward angular speed is 5°/s and the maximum reverse angular speed is $-2$°/s. Although there are multiple fluctuations in angular velocity during a single rotation cycle, the amplitude of the fluctuations is very small and the trend is gradual. According to Fig. 13 (c), if we remove some random points (which may be caused by tiny vibrations), the angular acceleration is between $-5°/s^2$ and $5°/s^2$, which contains large noise due to the slow angular velocity.

#### 1) ROTATION ANGLE MEASUREMENT RESULTS

Fig. 14 shows the estimated rotation angles of different methods in static situation. Part *A* is enlarged in Fig. 15. And Fig. 16 displays the static errors of rotation angle. As can be seen from them, the proposed IOE algorithm has a better static performance compared to the SORA and Zheng's algorithms with the maximum static error less than 1°. Since only the gyroscope is used to estimate the rotation angle, the drift of the gyroscope causes a large accumulated error later in the SORA method. Zheng's algorithm has a better performance in high-speed rotation compared to low-speed rotation. To show the best performance of the Zheng's algorithm when the rotation velocity is slow, we choose the relatively optimal rotating-axis estimation in the static experiment to estimate the rotation angle.

#### 2) ROTATING-AXIS MEASUREMENT RESULTS

Fig. 17 shows the estimated rotating-axis attitude components of X, Y and Z axis in the static performance experiment. Similarly, we take the Y-axis component of rotating-axis estimation in Fig. 17 (b) as an example to analyze. At the beginning and ending measurements, the rotation angle is close to zero, which leads to the inaccurate rotating-axis measurements of the IOE and SORA methods as shown in parts *A* and *G*. Once the rotation angle is greater than the threshold, the IOE and SORA methods could provide an accurate estimation of the rotation axis. Although the rotating-axis estimation of SORA method remains stable when the rotation angle is greater than the threshold, it will deviate from the actual rotation axis gradually as the drift errors of the gyroscope have not been eliminated. In Zheng's algorithm, the estimated rotating-axis attitude will distort significantly when the angular velocity is close to zero such

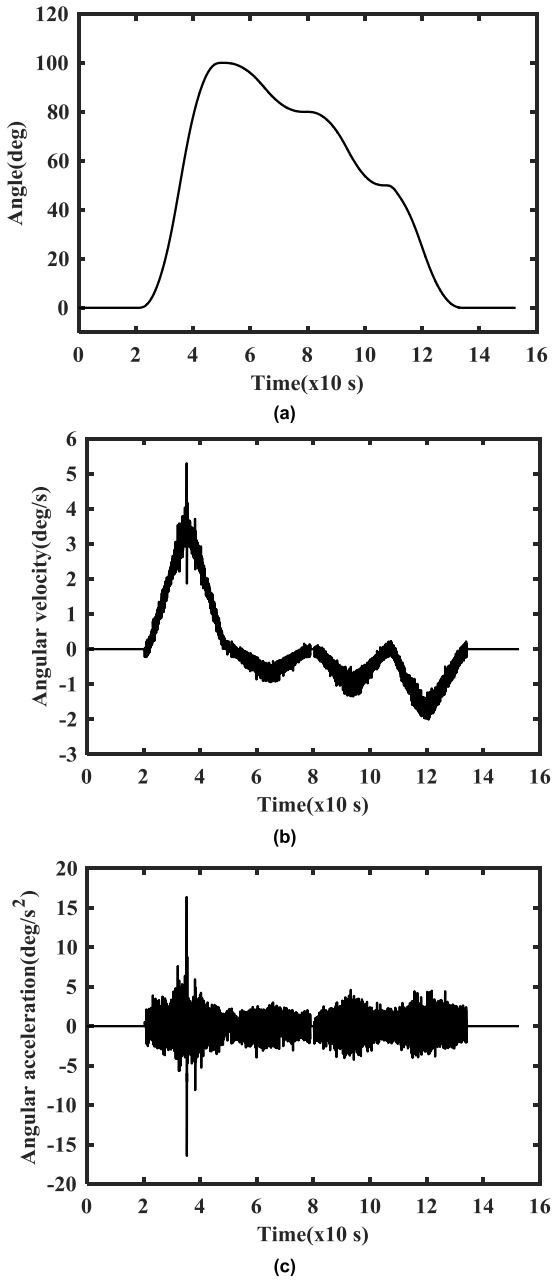


**FIGURE 13. The angles, angular velocity and angular acceleration curves of servo motor in static experiment. (a) Rotation angles; (b) Angular velocity; (c) Angular acceleration.**

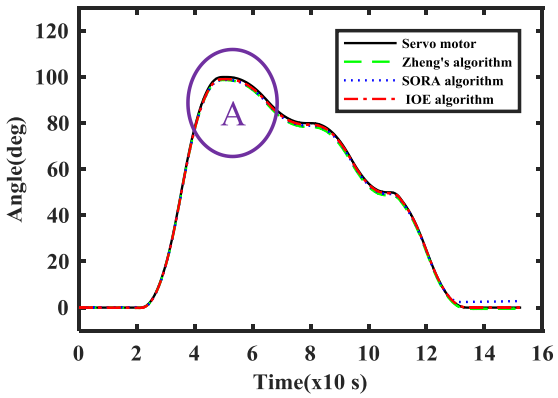


**FIGURE 14.** Estimated rotation angles in the static experiment.

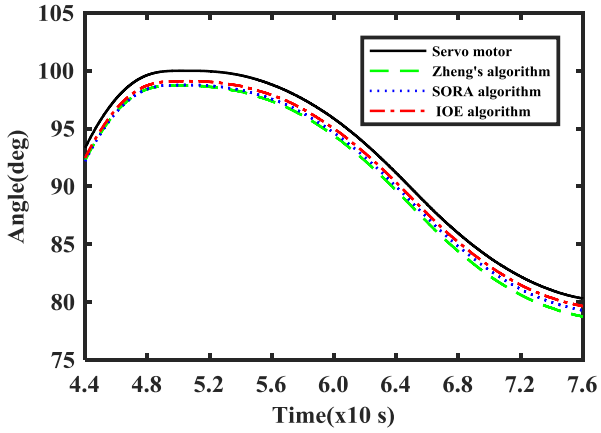


**FIGURE 15.** Magnification of part A in Fig. 14.

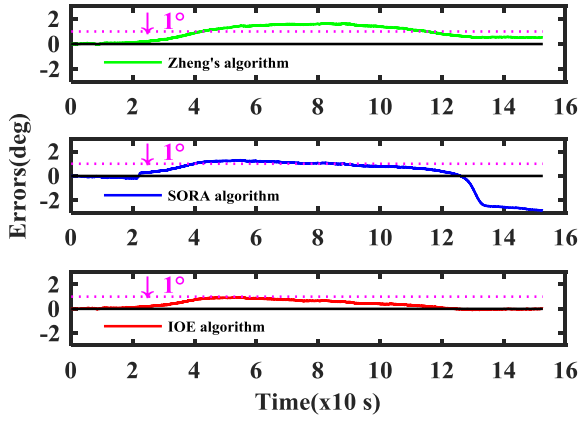


**FIGURE 16.** Static estimation errors of rotation angle.

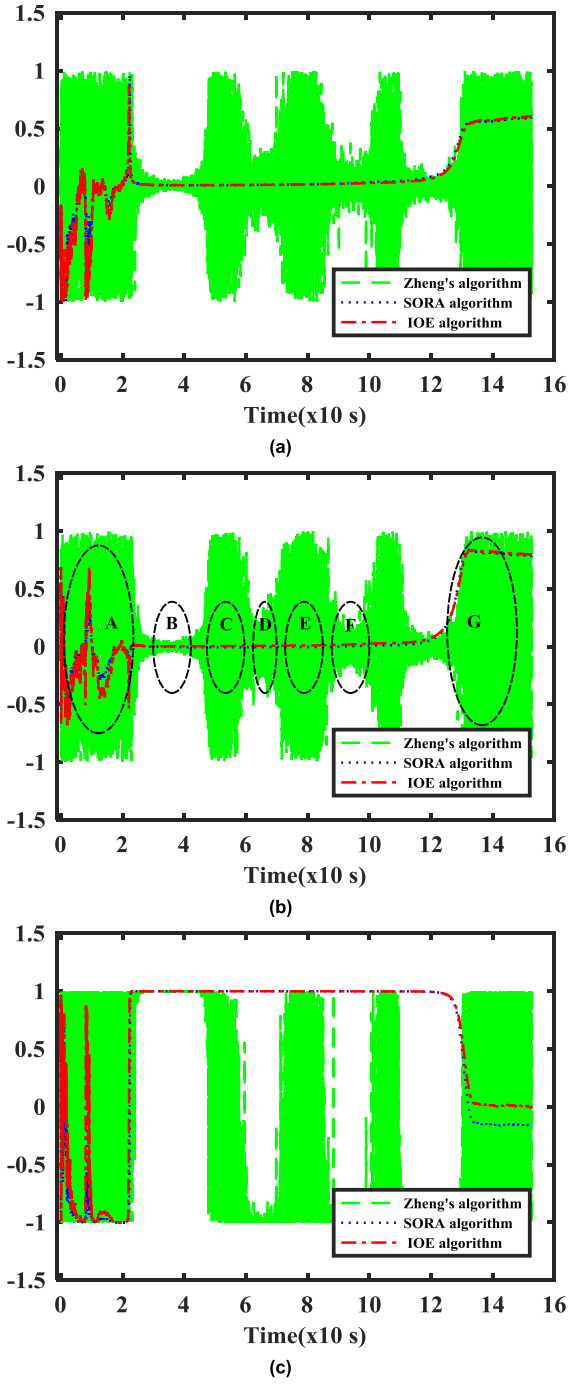


**FIGURE 17.** The estimated rotating-axis attitude in static test. (a) X axis; (b) Y axis; (c) Z axis.

as parts $A$, $C$, $E$ and $G$, which is similar to the dynamic performance experiments. It could not measure the rotation axis effectively in static experiments due to the small rotation velocity of the servo motor leads to a large proportion of noises contained in the angular velocity of the gyroscope. Thus, even the rotating-axis attitude tends to be stable in parts $B$, $D$ and $F$, they are not the accurate rotating-axis attitude.

Table 2 shows the RMSE of the rotation angle and axis in the static performance experiments, which indicates that the proposed IOE algorithm is more accurate compared to the other two methods.

We also calculate the average execution time of the three methods by running on an Intel core I5, 2.3 GHz processor. Results show that the average running time of Zheng's algorithm is 127.24$\mu$s, and the average running time of SORA

**TABLE 2. The static RMSE of rotation angle and axis.**

| RMSE | Zheng's algorithm | SORA algorithm | IOE algorithm |
|---|---|---|---|
| $\theta$ | 0.544° | 0.539° | 0.299° |
| ${}^{n}r_x$ | 0.0632 | $1.087\times10^{-3}$ | $2.223\times10^{-4}$ |
| ${}^{n}r_y$ | 0.0632 | $1.621\times10^{-3}$ | $1.694\times10^{-4}$ |
| ${}^{n}r_z$ | 0.0477 | $6.041\times10^{-6}$ | $2.378\times10^{-6}$ |

algorithm is 64.68$\mu$s. The running time of the proposed algorithm is 75.97$\mu$s. Obviously, the SORA algorithm and the proposed incremental-quaternion-based algorithm have higher computational efficiency compared to Zheng's algorithm whose computational complexity is almost twice than that of the other two algorithms. Therefore, the SORA algorithm and the incremental-quaternion-based algorithm are suitable to be implemented in the embedded systems.

## VI. CONCLUSIONS AND DISCUSSIONS

The main contributions of this work are that we design a compact MARGs-based measurement unit and propose a robust incremental-quaternion-based angle and axis estimation algorithm of single-axis rotation. It has the following advantages.

1) The incremental-quaternion is utilized to estimate the rotation angle and axis, which successfully avoids the gimbal lock problem in the Euler-angles-based algorithms. The proposed algorithm could achieve full-range rotation angle and all-attitude rotation axis measurements.
2) The proposed algorithm measures the rotation angle and axis using the information of MARG sensors, which eliminates the drift errors in the gyroscope-based or IMU-based measurements.
3) It has good performances on the rotation angle and axis estimation when the measured target is in dynamic or static movement.
4) With a small size of 30mm × 30mm × 10mm, the designed MARGs-based measurement unit simplifies the measurement process and reduces the measurement system's installation complexity. It has no restriction on installation methods and equipment, which is especially suitable for the situations where the traditional measurement equipment is difficult to install. For instance, the designed measurement unit and proposed algorithm could be utilized to measure the rotation angle of wheels, steering wheels and Ferris wheels *et al*. or calibrate the rotation angle of rudders of the ship, aircraft and UAVs.

The dynamic and static experiments show that the designed measurement unit and proposed algorithm could provide a robust estimation of rotation angle and axis of the single-axis rotation with high computational efficiency. The rotation angle estimation has the static error $< 1°$, dynamic error $< 2°$, static RMSE $< 0.4°$ and dynamic RMSE $< 0.3°$. In the rotating-axis attitude measurement, the dynamic error is less than $2.5\text{x}10^{-4}$ and the static error is less than 0.06. In the future, we will measure the rotation angle of joints of the robotic arm, in which the measurement will be more difficult due to the rotating-axis is time-varying. To achieve a more accurate rotation estimation of joints, it is necessary to estimate the rotating-axis attitude in real time. It may be an interesting and meaningful study.

## ACKNOWLEDGMENT

The authors would like to appreciate Yujie Sun's contributions on STM32 programming.

## REFERENCES

[1] D. Tick, A. C. Satici, J. Shen, and N. Gans, "Tracking control of mobile robots localized via chained fusion of discrete and continuous epipolar geometry, IMU and odometry," *IEEE Trans. Cybern.*, vol. 43, no. 4, pp. 1237–1250, Aug. 2013.
[2] H. Sekiya, T. Kinomoto, and C. Miki, "Determination method of bridge rotation angle response using MEMS IMU," *Sensors*, vol. 16, no. 11, pp. 1882–1894, 2016.
[3] A. Giannitrapani, N. Ceccarelli, F. Scortecci, and A. Garulli, "Comparison of EKF and UKF for spacecraft localization via angle measurements," *IEEE Trans. Aerosp. Electron. Syst.*, vol. 47, no. 1, pp. 75–84, Jan. 2011.
[4] E. Vinande, P. Axelrad, and D. Akos, "Mounting-angle estimation for personal navigation devices," *IEEE Trans. Veh. Technol.*, vol. 59, no. 3, pp. 1129–1138, Mar. 2010.
[5] N. A. Razak, N. H. M. Arshad, R. Adnan, M. F. Misnan, N. M. Thamrin, and S. F. Mahmud, "A real-time angle deviation detection and measurement technique for straight line quadrocopter navigation using accelerometer," in *Proc. IEEE Conf. Syst. Process Control (ICSPC)*, Kuala Lumpur, Malaysia, Dec. 2013, pp. 295–300.
[6] P. Müller, M.-A. Bégin, T. Schauer, and T. Seel, "Alignment-free, self-calibrating elbow angles measurement using inertial sensors," *IEEE J. Biomed. Health Inform.*, vol. 21, no. 2, pp. 312–319, Mar. 2017.
[7] C. Guo, D. Chen, C. Shen, Y. Lu, and H. Liu, "Optical inclinometer based on a tilted fiber Bragg grating with a fused taper," *Opt. Fiber Technol.*, vol. 24, pp. 30–33, Aug. 2015.
[8] A. Boboc and L. Zabeo, "Simultaneous cotton-mouton and faraday rotation angle measurements on JET," *Rev. Sci. Instrum.*, vol. 77, no. 10, pp. 10F324-1–10F324-4, 2006.
[9] H. Kim, Y. Yamakawa, T. Senoo, and M. Ishikawa, "Visual encoder: Robust and precise measurement method of rotation angle via high-speed RGB vision," *Opt. Express*, vol. 24, no. 12, pp. 13375–13386, 2016.
[10] S. Zheng, H. Dong, R. Zhang, Z. Huang, and J. Wang, "Angle estimation of a single-axis rotation: A practical inertial-measurement-unit-based method," *IET Sci. Meas. Technol.*, vol. 11, no. 7, pp. 892–899, Oct. 2017.
[11] J.-H. Pyo and K. Kim, "Precise angle estimation using geometry features for bin picking," in *Proc. IEEE Int. Conf. Adv. Robot. (ICAR)*, Hong Kong, Jul. 2017, pp. 281–283.
[12] J. Zhong, S. Zhong, Q. Zhang, Z. Peng, S. Liu, and Y. Yu, "Vision-based measurement system for instantaneous rotational speed monitoring using linearly varying-density fringe pattern," *IEEE Trans. Instrum. Meas.*, vol. 67, no. 6, pp. 1434–1445, Jun. 2018.
[13] B. Barshan and H. F. Durrant-Whyte, "Inertial navigation systems for mobile robots," *IEEE Trans. Robot. Autom.*, vol. 11, no. 3, pp. 328–342, Jun. 1995.
[14] E. de Souza Gonçalves and P. F. F. Rosa, "Cointegration analysis for IMU in a fixed-wing UAV," in *Proc. IEEE Int. Conf. Ind. Technol (ICIT)*, Toronto, ON, Canada, Mar. 2017, pp. 755–760.
[15] X. Chen, Y. Cai, Y. Ren, X.-D. Yang, and C. Peng, "Spacecraft angular rates and angular acceleration estimation using single-gimbal magnetically suspended control moment gyros," *IEEE Trans. Ind. Electron.*, to be published, doi: 10.1109/TIE.2018.2826468.
[16] R. E. Kalman, "A new approach to linear filtering and prediction problems," *Trans. ASME, D, J. Basic Eng.*, vol. 82, pp. 35–45, 1960.
[17] X. Tong *et al.*, "Adaptive EKF based on HMM recognizer for attitude estimation using MEMS MARG sensors," *IEEE Sensors J.*, vol. 18, no. 8, pp. 3299–3310, Apr. 2018.

[18] J.-P. Condomines, C. Seren, and G. Hattenberger, "Invariant unscented Kalman filter with application to attitude estimation," in *Proc. IEEE 56th Annu. Conf. Decis. Control (CDC)*, Melbourne, VIC, Australia, Dec. 2017, pp. 2783–2788.
[19] W. W.-L. Li, R. A. Iltis, and M. Z. Win, "Integrated IMU and radiolocation-based navigation using a Rao–Blackwellized particle filter," in *Proc. IEEE Int. Conf. Acoust. Speech Signal Process (ICASSP)*, Vancouver, BC, Canada, May 2013, pp. 5165–5169.
[20] S. O. H. Madgwick, A. J. L. Harrison, and A. Vaidyanathan, "Estimation of IMU and MARG orientation using a gradient descent algorithm," in *Proc. IEEE Int. Conf. Rehabil. Robot. (ICORR)*, Zurich, Switzerland, Jun./Jul. 2011, pp. 1–7.
[21] R. Mahony, T. Hamel, and J.-M. Pflimlin, "Nonlinear complementary filters on the special orthogonal group," *IEEE Trans. Autom. Control*, vol. 53, no. 5, pp. 1203–1218, Jun. 2008.
[22] W. Li, J. Jin, X. Li, and B. Li, "Method of rotation angle measurement in machine vision based on calibration pattern with spot array," *Appl. Opt.*, vol. 49, no. 6, pp. 1001–1006, 2010.
[23] J. Jin, L. Zhao, and S. Xu, "High-precision rotation angle measurement method based on monocular vision," *J. Opt. Soc. Amer. A, Opt. Image Sci.*, vol. 31, no. 7, pp. 1401–1407, 2014.
[24] S. Stančin and S. Tomažič, "Angle estimation of simultaneous orthogonal rotations from 3D gyroscope measurements," *Sensors*, vol. 11, no. 9, pp. 8536–8549, 2011.
[25] J. J. Craig, "Introduction," in *Introduction to Robotics*, 3rd ed. Beijing, China: China Machine Press, 2005, pp. 1–16.
[26] J. B. Kuipers, *Quaternions and Rotation Sequences*. Princeton, NJ, USA: Princeton Univ. Press, 1999, pp. 127–143.
[27] J. Diebel, "Representing attitude: Euler angles, unit quaternions, and rotation vectors," *Matrix*, vol. 58, nos. 15–16, pp. 10–11, 2006.
[28] O. Sarbishei, "On the accuracy improvement of low-power orientation filters using IMU and MARG sensor arrays," in *Proc. IEEE Int. Symp. Circuits. Syst. (ISCAS)*, Montreal, QC, Canada, May 2016, pp. 1542–1545.

**XIAOLONG XU** received the M.S. degree in mechanical design and theory from the Beijing University of Chemical Technology, Beijing, China, in 2014. He is currently pursuing the Ph.D. degree with the School of Control Science and Engineering, Shandong University, Jinan, China. His research interests include the robot, embedded systems, and wearable devices applied to human–robot collaboration.

**XINCHENG TIAN** received the B.Eng. and M.Eng. degrees in industrial automation from Shandong University, Jinan, China, in 1993 and 1988, respectively, and the Ph.D. degree in guidance, control, and simulation from the Nanjing University of Aeronautics and Astronautics, Nanjing, China, in 2000.

He is currently a Professor with the School of Control Science and Engineering, Shandong University. His main researches are the robot control technology, intelligent control of electromechanical system, and computer control technology and application.

**LELAI ZHOU** received the B.Eng. degree in mechanical engineering and automation from the University of Science and Technology Beijing, China, in 2006, the M.Eng. degree in mechanical design and theory from Beihang University, China, in 2009, and the Ph.D. degree in mechanical engineering from Aalborg University, Denmark, in 2012. He is currently an Associate Professor with the School of Control Science and Engineering, Shandong University. His main researches are robotic arm, human-centered design, and robotic exoskeletons.